J. Meas. Sci. Instrum., 2025, 16(2): 291-301. http://jmsi.publish.founderss.cn/
DOI: 10.62756/jmsi.1674-8042.2025028 jmsi@nuc.edu.cn

Fault diagnosis of railway switch machines based on VMD-SDP-CNN

SONG Yakun[1], FENG Qingsheng[1], XIAO Shuai[1], LI Hong[2*]

1. School of Electrical Engineering, Dalian Jiaotong University, Dalian 116028, China;
2. School of Railway Intelligent Engineering, Dalian Jiaotong University, Dalian 116028, China

***Corresponding author:** LI Hong (lihong@djtu.edu.cn)

Received: July 4, 2024 **Revised:** August 22, 2024 **Accepted:** September 23, 2024

Abstract: The switch machine is a vital component in the railway system, playing a significant role in ensuring the safe operation of trains. To address the shortcomings of existing fault diagnosis methods for the switch machine and leveraging the strong anti-interference and high sensitivity characteristics of vibration signals, we proposed a VMD-SDP-CNN (Variational mode decomposition-Symmetric dot pattern-Convolutional neural network) fault diagnosis method based on switch machine vibration signals. Firstly, the vibration signal of the switch machine was decomposed by VMD to obtain several intrinsic mode function (IMF) components. Secondly, the SDP method was employed to transform the decomposed IMF components into two-dimensional images, and the issue of one-dimensional signal recognition was transformed into the issue of two-dimensional image recognition. Finally, a CNN was used to realize the fault diagnosis of the switch machine. The experimental results showed that the recognition accuracy of the five actual working conditions of the switch machine using this method was superior to that of typical deep learning and machine learning methods, verifying its practicability and effectiveness.

Key words: switch machine; rail transit; turnout; intelligent diagnosis; vibration signal; signal decomposition; deep learning

0 Introduction

The rail transit system has developed rapidly, with switch machines being widely deployed as turnout conversion devices. Due to their complex working environments and high frequency of operation, they often malfunction. Up to now, the popular fault diagnosis methods of the switch machine mainly rely on manually reviewing the power curves of the switch machine recorded by the railway centralized signaling monitoring system. This approach not only requires a significant amount of manual work but also easily causes missed and false detection[1]. By introducing machine learning and data analysis techniques, automatic processing of large amounts of monitoring data and identification of fault modes can be achieved, thereby improving the accuracy and efficiency of diagnosis[2].

Scholars have conducted thorough research on intelligent diagnosis methods for the switch machine. Zhang et al.[3] proposed a fault identification algorithm for speed-up turnouts based on the BP neural network. The feature vector values extracted from the action current curve of the switch machine can be accurately and effectively mapped to the fault type. A method based on energy-based threshold wavelet (EBTW) was proposed to extract the time-frequency characteristics of the switch machine current signal, which significantly improved the accuracy of turnout fault detection under different fault severity[4]. Reetz et al.[5] presented a Bayesian network model that diagnosed railway point machine faults by combining expert knowledge with limited data to support maintenance decision-making. Sugiana et al.[6] developed a cost-effective fault diagnosis method for railway point machines using time-series data extracted through time-domain feature extraction and scalable hypothesis testing. Lao et al.[7] proposed an improved LightGBM-based fault diagnosis method for turnout switch machines, using time domain features, multi-scale permutation entropy, and an adaptive feature selection method to enhance diagnostic accuracy. Shi et al.[8] introduced an enhanced fault diagnosis method for ZDJ7 railway point machines using improved DCNN and SVDD, achieving high accuracy with robust performance against noise and unbalanced features.

The research objects of the switch machine fault diagnosis mainly focus on electrical signals, including current and power curves. However, these methods lack sufficient sensitivity for some specific types of faults, such as wear or looseness of mechanical components. The use of electrical signals fault diagnosis methods lacks sufficient sensitivity, and it is difficult to detect problems promptly.

Some scholars have begun to analyze the switch machine from other perspectives. Lee et al.[9] used audio data of the switch machine, but there were often a variety of noises on the railway site that adversely affected the detection. Zhou et al.[10] and Yang et al.[11] used oil pressure data of the switch machine, but this method was only applicable to the electro-hydraulic switch machine. Cao et al.[12] and Sun et al.[13] proposed a method for fault detection and recognition using the vibration signal of the switch machine, which was a new perspective. The vibration signal can embody small vibrations during the operation of the switch machine, making it highly sensitive to the machine's operating state and internal structural changes, thereby providing more detailed and accurate information. Therefore, we chose the vibration signal of the switch machine as the research object.

Variational mode decomposition (VMD) was a time-domain signal analysis method[14]. Compared to the earlier empirical mode decomposition (EMD) method[15], VMD avoids endpoint effects and mode mixing problems[16]. It has a solid mathematical foundation, which helps to reduce the complexity of highly complex and strongly nonlinear time series. The symmetric dot pattern (SDP) method protrudes signal characteristics by transforming one-dimensional signals into two-dimensional images[17]. This method is often used in combination with deep learning and has been applied in the field of mechanical vibration, including bearings[18,19], permanent magnet synchronous motors[20], and reciprocating compressors[21]. Convolutional neural network (CNN) holds significant advantages in the field of image processing due to its specialized architecture[22]. Lü et al.[23] employed optimized VMD and continuous wavelet transform (CWT) for vibration signal preprocessing, followed by CNN for classifying valve plate wear states. Zhang et al.[24] converted the one-dimensional current signal of the switch machine into the two-dimensional grayscale image and employed CNN for fault classification, achieving satisfied results.

However, the one-dimensional vibration signals of power on and off have not yet been studied to be converted into two-dimensional images to discover more features of the signals. Therefore, combined with the vibration data of the switch machine, this paper proposes a fault diagnosis method for the switch machine based on VMD-SDP-CNN. Firstly, the vibration signal during the operation of the switch machine was decomposed using VMD to obtain several IMF components. These IMF components were then transformed from one-dimensional signals to two-dimensional images using the SDP method. Finally, the SDP image was used as CNN input to realize the identification and classification of the working state of the switch machine.

1 VMD-SDP-CNN

1.1 VMD

VMD can retain the important information in the original signal during the signal decomposition process and suppress irrelevant or noise components, making the decomposed IMF components better reflect the characteristics of the signal. Using VMD to process the signal, the center frequency and limited bandwidth of each mode can be adaptively matched, and the signal decomposition can be realized by solving the best solution of the constrained variational model[25]. The solving steps are as follows.

For each component $u_k(t)$, Hilbert transform[26] is performed to obtain the analytical signal and spectrum of the signal. And for each analytic signal, it is multiplied by an exponential term $e^{-j\omega_k t}$, i.e.,

$$\left[\left(\delta(t)+\frac{j}{\pi t}\right)u_k(t)\right]e^{-j\omega_k t}. \tag{1}$$

By modulating the signal and calculating the gradient norm, the center frequency bandwidth of the modal component can be estimated. This process transforms VMD into a constrained variational problem. In this variational problem, the constraint condition is that the sum of each component is equal to the signal f to be separated, and the sum of the estimated bandwidth of each component is the smallest.

$$\min_{\{u_k\}\{w_k\}}\left\{\sum_k\left\|\partial_t\left[\left(\delta(t)+\frac{j}{\pi t}\right)u_k(t)\right]e^{-jw_k t}\right\|_2^2\right\},\quad \text{s.t.}\sum_k u_k=f, \tag{2}$$

where $\delta(t)$ is the pulse function; f is the input signal; $u_k(t)$ is the k IMF components obtained by signal decomposition; w_k is the center frequency of each IMF component.

Combining the objective function with the constraint condition, the augmented Lagrange expression is constructed, including the objective function and the constraint term. At the same time, the Lagrange multiplier $\lambda(t)$ is introduced to represent the penalty term of the constraint condition. An unconstrained variational problem containing only component parameters is obtained.

$$L(\mu_k,\omega_k,\lambda)=\alpha\sum_k\left\|\partial_t\left[\left(\delta(t)+\frac{j}{\pi t}\right)u_k(t)\right]e^{-j\omega_k t}\right\|_2^2+\left\|f(t)-\sum_k u_k\right\|_2^2+\left\langle\lambda(t),f(t)-\sum_k u_k(t)\right\rangle, \tag{3}$$

where α is the penalty factor; $\lambda(t)$ is the Lagrange multiplier.

To determine the best solution for the constrained variational equation, the alternating multiplication operator is introduced to update u_k^{n+1}, w_k^{n+1}, and λ^{n+1}. In the process of solving the optimal value, the variable update formulas are

$$u_k^{n+1}(\omega)=\frac{f(\omega)-\sum_{i\neq k}u_i^n(\omega)+0.5\lambda(\omega)}{1+2\alpha(\omega-\omega_k)^2}, \tag{4}$$

$$w_k^{n+1}=\frac{\int_0^\infty \omega|u_i^n(\omega)|^2\mathrm{d}\omega}{\int_0^\infty |u_i^n(\omega)|^2\mathrm{d}\omega}, \tag{5}$$

$$\lambda^{n+1}=\lambda^n+\tau\left(f(\omega)-\sum_k u_k^{n+1}(\omega)\right), \tag{6}$$

where n is the number of iterations; τ is the fidelity coefficient; $f(\omega)-\sum_k u_k^{n+1}(\omega)$ is the residue of signal decomposition; w_k^{n+1} and λ^{n+1} are constantly updated. The above steps are repeated and iterated until the conditions are met. Finally, the signal is successfully decomposed and multiple IMF components are obtained.

1.2 SDP

The generation principle of symmetrized dot pattern (SDP) image[27] is to transform a one-dimensional signal into a two-dimensional SDP image through the corresponding formula and express the fault information characteristics of the signal through the image. This method can directly convert non-stationary and non-linear signals into SDP images in polar coordinates, as shown in Fig.1. $r(i)$ is the polar radius of the polar coordinate, $\phi(i)$ and $\theta(i)$ represent the rotation angles in clockwise and counterclockwise directions.

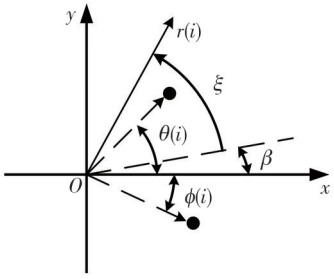

Fig. 1 SDP schematic diagram

A set of signals $X=\{x_1,x_2,\cdots,x_{n-1},x_n\}$ can be transformed into SDP images in polar coordinates according to the above parameters. The specific calculation formulas of the three parameters are

$$r(i)=\frac{x_i-x_{\min}}{x_{\max}-x_{\min}}, \tag{7}$$

$$\theta(i)=\beta+\frac{x_{i+l}-x_{\min}}{x_{\max}-x_{\min}}\xi, \tag{8}$$

$$\phi(i)=\beta-\frac{x_{i+l}-x_{\min}}{x_{\max}-x_{\min}}\xi, \tag{9}$$

where $x_{\max}$ and $x_{\min}$ are the maximum and minimum of the selected signal X, respectively; x_i is the ith sample point of the signal; l is the time interval parameter, and it will affect the shape of the pattern; β is the symmetric rotation initial angle, and the pattern will be symmetrically generated on both sides of this angle; ξ is the angle amplification factor, which determines the separation and convergence of patterns.

1.3 CNN

CNN is a typical deep-learning neural network[28]. Its essence is to construct hierarchical feature representation through convolution operation and pooling operation, so as to realize effective representation learning and pattern recognition of input data. As shown in Fig.2, a normal CNN usually takes the convolution layer as the first layer, and the pooling layer is usually set after the convolution layer. Through the stacking of multi-layer convolutional layers and pooling layers, and finally through the fully connected layer, the feature representation is mapped to the output category.

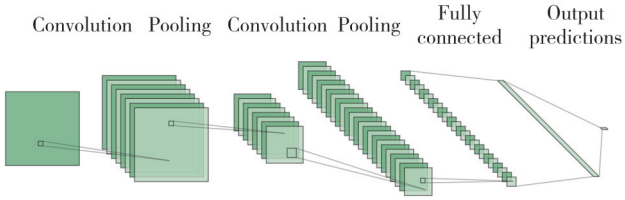

Fig. 2 CNN structure diagram

In CNN, the convolutional layer extracts local features by sliding the convolution kernel over the input data to generate a feature map. The pooling layer reduces the spatial dimensions of the feature map, decreases computational complexity, and retains the most significant features. By performing pooling operations, CNN can preserve crucial feature information and reduce the risk of overfitting. The fully connected layer maps the extracted high-level features to the final output category. This layer associates the feature vector with the output category, making it suitable for classification and regression tasks.

CNN has the characteristics of multi-level feature learning and weight sharing. Multi-level feature learning can extract more abstract and complex features. Weight sharing can improve the generalization ability of the model and reduce the occurrence of overfitting. In the training phase, CNN inputs the input data into the network through forward propagation, calculates the output results, and then updates the network parameters through the back propagation algorithm to minimize the error cost function, so as to adjust the network parameters until the network converges or reaches the iteration termination condition.

1.4 Diagnosis process

The process of the intelligent fault diagnosis method

for the switch machine proposed is shown in Fig.3.

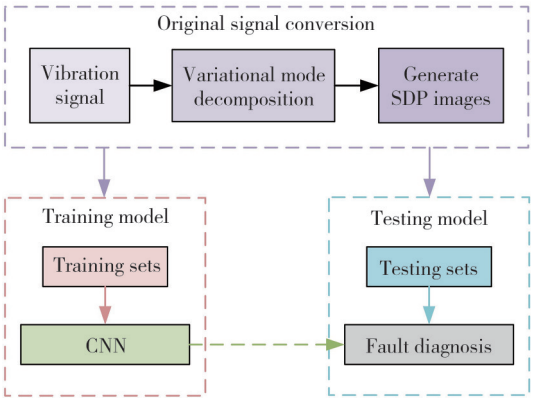

Fig. 3 Fault diagnosis process of switch machine

Step 1 Install the vibration sensor in an appropriate position on the switch machine, and collect vibration signals under different working conditions.

Step 2 Signal decomposition. Select an appropriate decomposition level K for VMD of the collected vibration signal, and decompose the signal into several IMF components.

Step 3 Transform the IMF components obtained after decomposition into two-dimensional images in polar coordinates using the SDP method, and select appropriate SDP parameters to amplify the signal differences.

Step 4 Build a CNN model and set its parameters, including the number of layers, convolution kernel size, pooling method, etc. Divide the data set and train the CNN with the training set data.

Step 5 Input the test set data into the trained CNN, review the test results, and achieve fault classification and diagnosis.

2 Experiments

2.1 Experimental data description

In this study, the ZD6 switch machine traction turnout of a railway training base was taken as the experimental object. The sensor adopted the WTVB01-485 three-axis vibration sensor, which was installed at the throwing rod of the ZD6 switch machine. The throwing rod connected the switch machine to the turnout and served as the carrier of the traction force. The torque of the switch machine motor was amplified by the reducer to drive the throwing rod to pull the turnout. Therefore, the vibration of the throwing rod can reflect the operating conditions of the switch machine. The vibration sensor was connected to a personal computer to collect and record the vibration signals of the switch machine. The switch machine was remotely controlled by the indoor console, and the vibration displacement signals of the five operating conditions of the switch machine were collected by the vibration sensor. The acquisition frequency is 1 kHz, and the acquisition time ranges from 7 to 9 s. Approximately 40 sets of data are collected for each working condition, resulting in a total of 204 sets of data. The descriptions of the five working conditions are provided in Table 1.

Table 1 Description of five working conditions of switch machine

Condition	Description	Number of samples
a	Normal operation	40
b	Turnout cannot be locked	38
c	Abnormal resistance exists in process of turnout conversion	42
d	Friction current is too small	40
e	Throwing rod is disconnected from turnout	44

The vibration sensor collects three sets of vibration signals in the X, Y, and Z triaxial directions by default. The X-axis and Y-axis vibration signals are actually the projections of the action rod's vibration along the sensor's X and Y axes. Therefore, the acquisition of X-axis and Y-axis vibration signals needs to ensure that the angle of the sensor installation is the same, which is inconvenient in actual operation. Consequently, it is decided to exclude the X-axis and Y-axis vibration signals from the study and focus solely on the Z-axis vibration signals. After standardizing the sample length to 7 000, the time-domain waveforms corresponding to each working condition are shown in Fig.4.

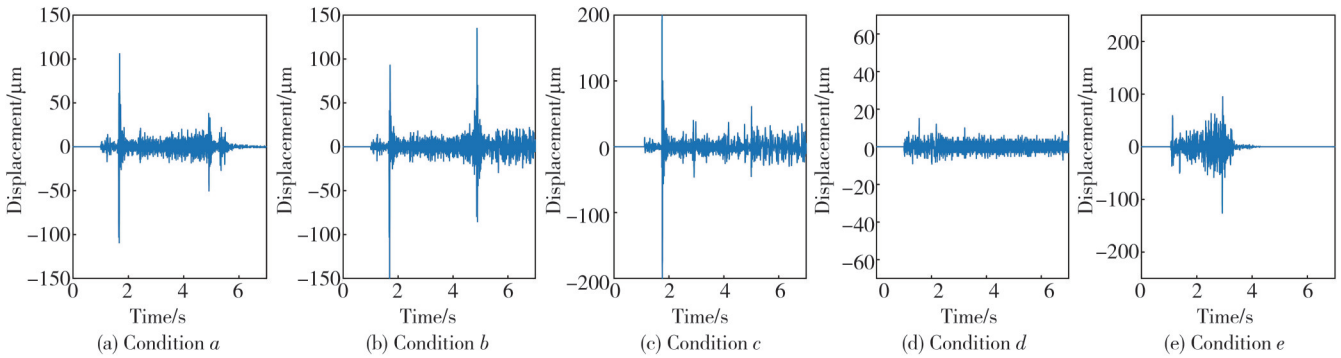

Fig. 4 Time-domain waveform of vibration signal under five working conditions

2.2 Vibration signal decomposition

When using VMD to decompose the signal, it is necessary to preset the number of decomposition layers K. K directly affects the validity of the decomposition. If the K value is too small, it may not be able to capture all the important frequency components, resulting in information loss. If the K value is too large, it may lead to important information being masked by irrelevant components in the decomposition results. Therefore, the center frequency method is used to determine the number of decomposition layers[29]. The difference between different IMF components mainly lies in the difference in center frequency, each IMF component corresponds to an independent frequency bandwidth.

Ideally, the center frequencies of different components should not overlap or be far away from each other, indicating that these components represent different frequency components in the signal. By comparing the center frequency of each IMF component under different decomposition layers, the value of the optimal decomposition layer K can be determined. We select one working condition d vibration signal and use VMD to decompose the signal. The decomposition results are shown in Table 2.

Table 2 IMF center frequency of different K values

K	IMF center frequency/Hz						
	IMF1	IMF2	IMF3	IMF4	IMF5	IMF6	IMF7
5	11.2	27.1	54	92.9	243.4	—	—
6	11.2	26.9	53.2	92.5	205.4	340.1	—
7	10.9	25.8	48.4	86.5	96	209.1	344.1

It can be seen that when the decomposition layer K is 7, the maximum center frequency of the decomposed IMFs is close to that when K is 6. This indicates that the vibration signal is over-decomposed, so the ideal value of K is determined to be 6. When the decomposition layer K is 6, VMD is used to decompose the vibration signal of five working conditions, as shown in Fig.5. The decomposed IMF components are ordered from high frequency to low frequency.

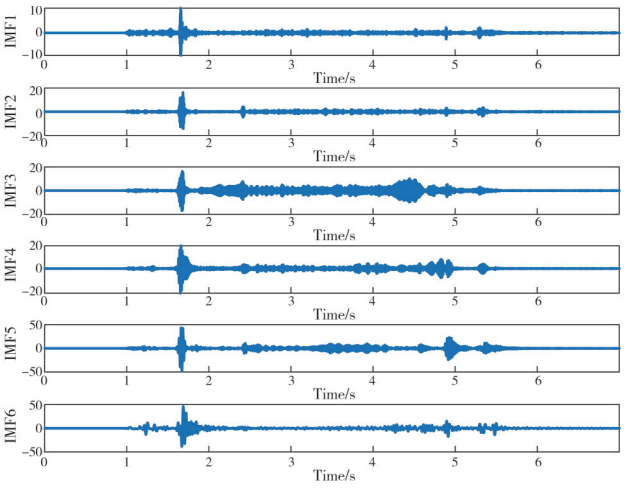

(a) Decomposition results of condition *a*

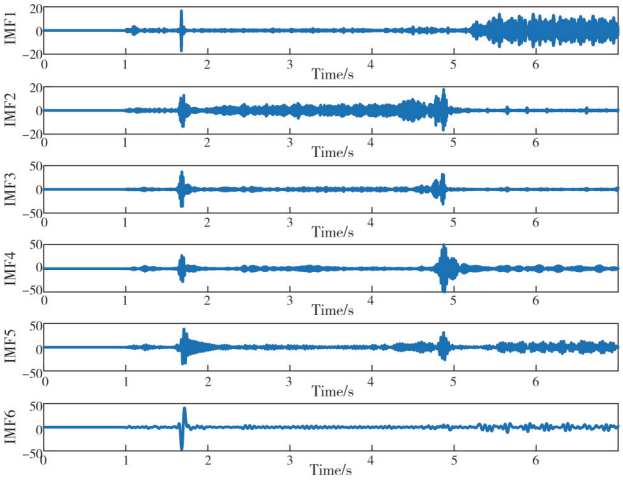

(b) Decomposition results of condition *b*

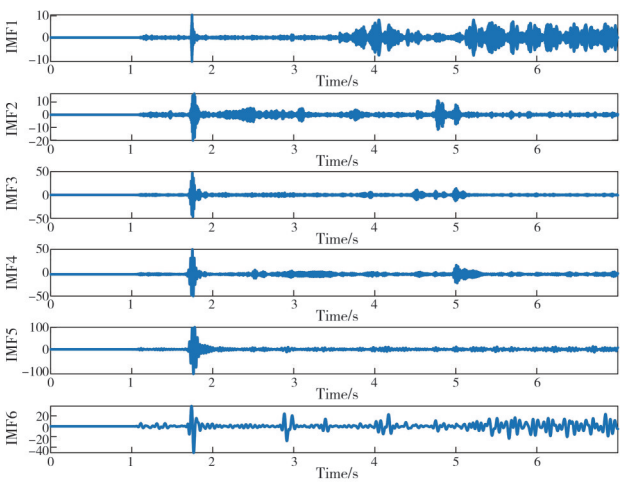

(c) Decomposition results of condition *c*

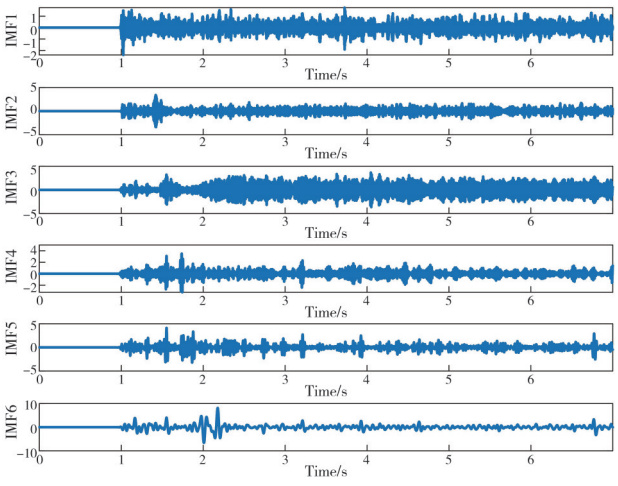

(d) Decomposition results of condition *d*

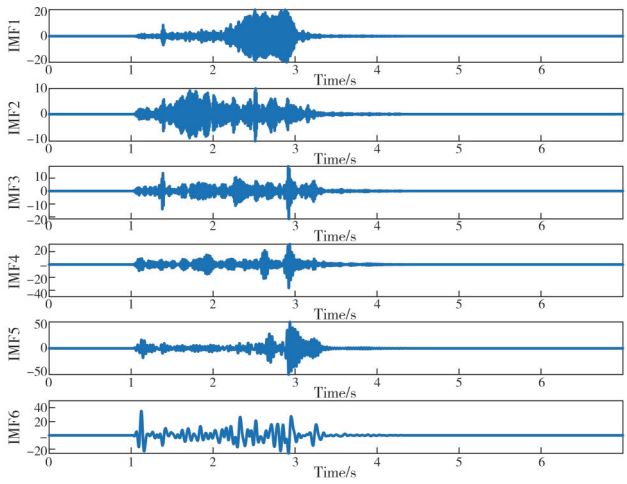

(e) Decomposition results of condition *e*

Fig. 5 IMF components obtained after vibration signal decomposition

2.3 SDP image conversion

In this section, the IMF components obtained by decomposing the vibration signal were transformed into a two-dimensional SDP image in polar coordinates by using the SDP method, and then the hidden features in the vibration signal were found. The selection of parameters in the SDP method is very important. If the parameters are not properly selected, the effect of generating pictures will be poor.

Angle amplification factor ξ determines the angle distribution range of petals. When adjusting the angle amplification factor ξ, it should be ensured that the SDP image can cover the entire coordinate system[30], and the images do not overlap too much. Because a total of six IMF components are involved in the transformation of the SDP diagram, the angle amplification factor ξ is set to $\frac{360}{6\times 2}=30$. The time interval parameter l affects the shape of the pattern. The value of this parameter is usually set between 1 and 20. When the value is set to 1, the pattern only looks like two lines. As the value increases, the pattern begins to spread from the side of the line, and finally it is like petals. At the same time, the differences between SDP images are gradually revealed. When selecting l, we need to comprehensively consider the difference between SDP images under different working conditions and the similarity of SDP images under the same working conditions. If we just blindly pursue the difference of SDP images under different working conditions, it may also cause a large difference in SDP images under the same working conditions, which ultimately leads to unsatisfactory fault classification results of the switch machine.

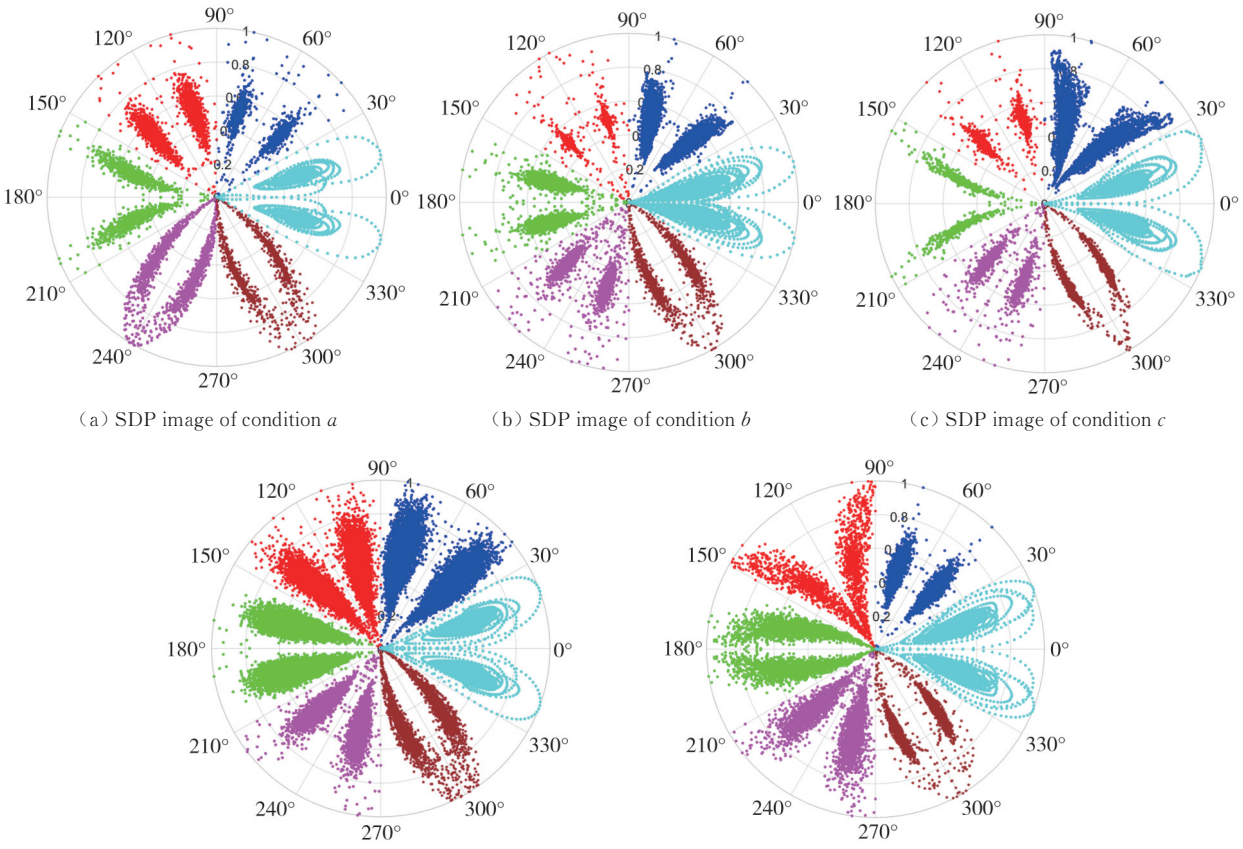

(a) SDP image of condition *a* (b) SDP image of condition *b* (c) SDP image of condition *c*

(d) SDP image of condition *d* (e) SDP image of condition *e*

Fig. 6 SDP images of five working conditions of switch machine

After several experiments, the time interval parameter l is finally determined to be 15. The six IMF components are plotted in polar coordinates, and the final SDP image is shown in Fig.6.

It can be seen that after selecting the appropriate parameters, there are obvious differences between the SDP images corresponding to different working conditions of the switch machine. Different faults uniquely influence the shape of the petal, effectively expressing the hidden fault features in the vibration signal of the switch machine.

2.4 Establishment of CNN model

The CNN model employed in this study employed the classic LeNet structure and was implemented using the PyTorch deep learning framework. The network consisted of three convolutional layers, three pooling layers, and fully connected layers. The model took SDP images as input and used a softmax classifier in the output layer. The ReLU function was used as the activation function, and max-pooling was applied in the pooling layers. Detailed parameter settings of the network model are presented in Table 3.

The dataset is divided into a training set and a testing set in a ratio of 7∶3. CNN models usually have a large number of parameters, which necessitates a sufficient proportion of samples for training to avoid issues such as overfitting and local optima[31]. Given the diversity of the switch machine types in real-world scenarios, the sample size for each specific type of switch machine fault is limited. To address this, we applied data augmentation techniques, including rotating SDP images and adding noise, which expanded the dataset from 204 to 2 040 samples.

Table 3 CNN model parameter settings

Layer	Kernel (high×wide/step)	Feature size
Input	—	224×224×3
Convolution1	3×3/1	224×224×16
Pooling1	2×2/2	112×112×16
Convolution2	3×3/1	112×112×32
Pooling2	2×2/2	56×56×32
Convolution3	3×3/1	56×56×64
Pooling3	2×2/2	28×28×64
Fully connected	—	64
Output	—	5

3 Results and discussion

The CNN model was trained and tested with a batch size of 16 for both training and testing. The cross-entropy loss function was chosen for loss calculation, and the Adam optimizer is used with an initial learning rate of 0.001. The number of training iterations is set to 40.

To validate fault diagnosis capability of the proposed method's, we utilized the t-SNE method to perform dimensionality reduction and visualization on the experiment result[32]. The objects include original one-dimensional signals, the two-dimensional SDP images (i.e., the input of the CNN), and the output of the CNN, as shown in Fig.7.

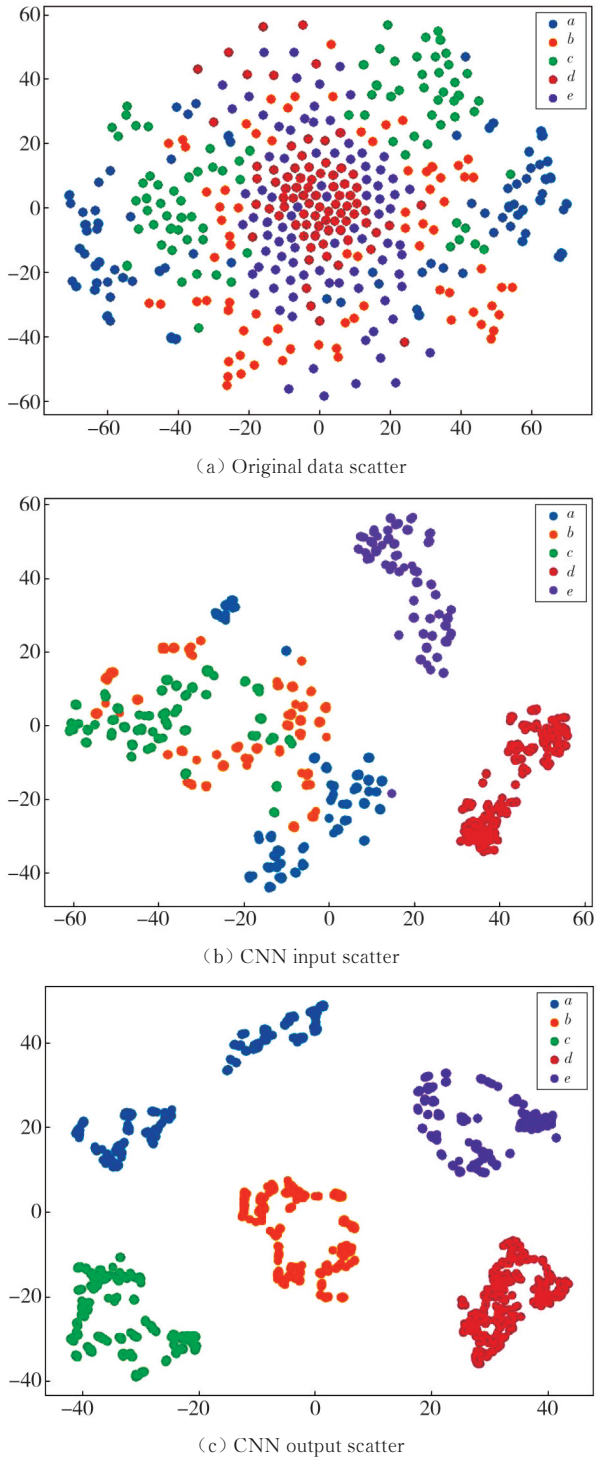

(a) Original data scatter

(b) CNN input scatter

(c) CNN output scatter

Fig. 7 Dimensionality reduction visualization results

It can be seen from Fig. 7(a) that the distribution of scatter plots generated by the original one-dimensional signal is overlapped and difficult to distinguish. It can be seen from Fig. 7(b) that after transforming the one-dimensional signal into SDP image, the characteristics of different working conditions of the switch machine are protruded, and the scatter points corresponding to the same working conditions begin to gather, but there are still three working conditions that have not been well distinguished. It can be seen from Fig. 7(c) that the scatter points of different working conditions are distributed in different regions of the space, and the discrimination is obvious, which proves the effectiveness of the CNN model in extracting SDP image features to realize the classification of switch machine working conditions.

The accuracy and loss curves of the model training are shown in Fig.8.

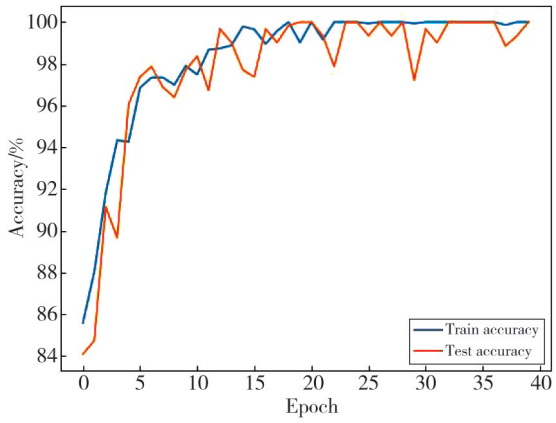

(a) Accuracy curves over epochs

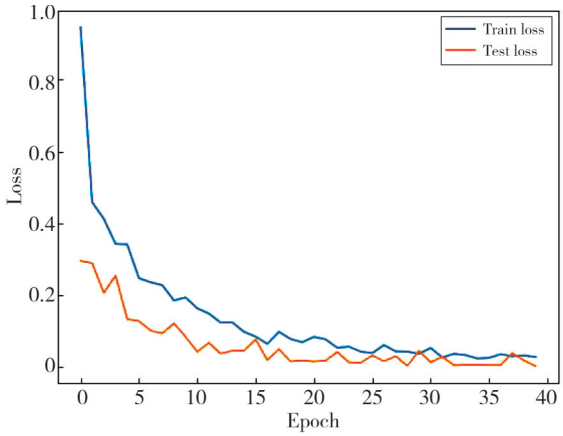

(b) Loss curves over epochs

Fig. 8 Training curves

It can be seen from Fig.8(a) that the training accuracy and test accuracy show a rapid upward trend in the early stage of training, and reach more than 95% accuracy around 10 rounds. As the number of rounds increases, the training curve tends to be stable, and the last two curves are very close, indicating that the model has high accuracy on both the training and test sets. It can be seen from Fig.8(b) that the training loss decreases rapidly in the first few rounds, indicating that the model effectively learns the characteristics of the data. After that, the loss curve slowly declines and eventually stabilizes. The test loss shows a similar downward trend. On the whole, the gap between the training and test loss curves is small, indicating that the model has good generalization ability.

The confusion matrix of one test result is shown in Fig. 9. The columns of the confusion matrix correspond to the actual category of the working condition, and the rows correspond to the predicted category of the working condition. And a—e represent the label of different working conditions of the switch machine, respectively. It can be seen that the classification results of the remaining working conditions are correct except that a small number of actual working condition b are mistakenly identified as working condition a. It can be observed that the accuracy of this test is 99.67%, which shows that the method proposed in this paper can accurately identify the five working conditions of the switch machine.

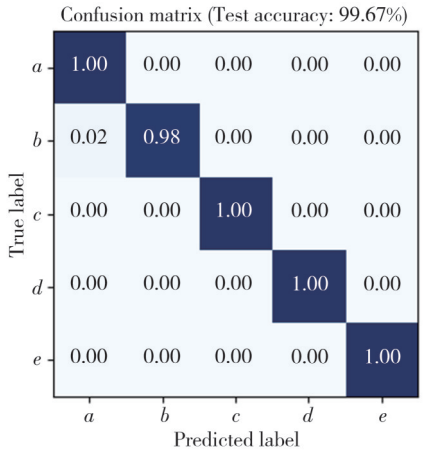

Fig. 9 Confusion matrix

3.1 Ablation study

This section performs ablation study on each module in the proposed method and trains the CNN model after removing one of the modules each time. To remove the influence of fortuitous factors, each experiment was performed 10 times, and the average accuracy of the 10 results was used to evaluate its performance. The average accuracy is shown in Table 4. It can be seen that the VMD-SDP-CNN method achieves an average accuracy of 99.7%. This composite signal processing method significantly outperforms the individual signal processing methods, SDP-CNN and VMD-CNN, in

terms of accuracy. This validates that the combined use of VMD and SDP methods contributes to better identification of the switch machine's status.

Table 4 Ablation experimental results

Model	Average accuracy/%
SDP-CNN	92.0
VMD-CNN	94.1
VMD-SDP-CNN	99.7

3.2 Comparative experiment

To further verify the effectiveness of the VMD-SDP-CNN method, we compared it with SVM, 1DCNN (one-dimensional convolutional neural network), RF (random forest), AFS (adaptive feature selection) - LightGBM[7], DRFF (deep random forest fusion) [11], and VMD-ReliefF-SVM[12] on the testing set. The final experimental results are shown in Table 5.

Table 5 Average accuracy of different diagnostic methods

Model	Average accuracy/%
SVM	88.5
1DCNN	91.8
RF	95.1
AFS-LightGBM	93.1
DRFF	96.7
VMD-ReliefF-SVM	95.2
VMD-SDP-CNN	99.7

It can be seen that the accuracy of SVM in classifying switch machine vibration signals is relatively low, at only 88.5%, which is lower than that of RF. Although the 1DCNN does not require manual feature extraction, its accuracy is not high either. The AFS-LightGBM method achieves an accuracy of 93.1% on this dataset. In contrast, the DRFF and VMD-ReliefF-SVM methods for switch machine vibration signals achieve accuracies of 96.7% and 95.2% on this dataset. The average diagnostic accuracy of the VMD-SDP-CNN method proposed in this paper is higher than that of the other six methods, indicating that the proposed method effectively identifies and classifies different working conditions of the switch machine.

4 Conclusions

The combination of VMD and SDP signal processing methods transformed one-dimensional vibration signals into two-dimensional images to protrude fault features. Then these images served as inputs to CNN to classify various operating conditions of the switch machine, realizing intelligent fault diagnosis. The vibration signal was easy to collect, making it applicable to various types of switch machines. This study focused on the vibration signal of the ZD6 switch machine collected in the actual field, demonstrating the practicability of this method. The VMD-SDP-CNN method achieved precise diagnosis of different faults, boasting a diagnostic accuracy of 99.7%, thus confirming its effectiveness. Furthermore, this research represented a novel exploration into the application of deep learning within rail transit.

In the follow-up study, we will consider the challenges that may be encountered in the practical application of the theoretical method. For example, in the actual railway environment, the vibration of the train on the rail will also affect the switch machine, which will put forward higher requirements for intelligent algorithms. And improving the interpretability of the deep learning method in the field of the switch machine is also our research focus.

Acknowledgement

This work was supported by Scientific Research Project of the Education Department of Liaoning Province (No. JYTMS20230008) and Scientific Research Project of Transportation Department of Liaoning Province (No.202320).

Declaration of conflicting interests

The authors have no conflict of interests related to this publication.

References

[1] HU X, TANG T, TAN L, et al. Fault detection for point machines: a review, challenges, and perspectives. Actuators, 2023, 12(10): 391.

[2] HU X, CAO Y, TANG T, et al. Data-driven technology of fault diagnosis in railway point machines: review and challenges. Transportation Safety and Environment, 2022, 4(4): tdac036.

[3] ZHANG K, SONG J, JU Y. Algorithm of speed-up turnout indication circuit fault intelligent diagnosis//2015 8th International Symposium on Computational Intelligence and Design (ISCID), December 12-13, 2015, Hangzhou, China. New York: IEEE, 2015: 551-554.

[4] CHEN Q, NICHOLSON G, ROBERTS C, et al. Improved fault diagnosis of railway switch system using energy-based thresholding wavelets (EBTW) and neural networks. IEEE Transactions on Instrumentation and Measurement, 2020, 70: 3503312.

[5] REETZ S, NEUMANN T, SCHRIJVER G, et al. Expert system based fault diagnosis for railway point machines. Proceedings of the Institution of Mechanical Engineers, Part F: Journal of Rail and Rapid Transit,

2024, 238(2): 214-224.
[6] SUGIANA A, CAHYADI W A, YUSRAN Y. Current-signal-based fault diagnosis of railway point machines using machine learning. Applied Sciences, 2024, 14(1): 267.
[7] LAO Z, HE D, WEI Z, et al. Intelligent fault diagnosis for rail transit switch machine based on adaptive feature selection and improved LightGBM. Engineering Failure Analysis, 2023, 148: 107219.
[8] SHI Z, DU Y, YAO X. Fault diagnosis of ZDJ7 railway point machine based on improved DCNN and SVDD classification. IET Intelligent Transport Systems, 2023, 17(8): 1649-1674.
[9] LEE J, CHOI H, PARK D, et al. Fault detection and diagnosis of railway point machines by sound analysis. Sensors, 2016, 16(4): 549.
[10] ZHOU J, LI Y, LI S. Railway perimeter monitoring system based on optical fiber vibration sensor and video analysis technology. Railway Signalling & Communication, 2019, 55(4): 52-55.
[11] YANG X, WANG Z, HUANG J, et al. Fault diagnosis of switch machine based on visibility graph feature and CatBoost. Journal of North University of China (Natural Science Edition), 2024, 45(1): 58-65.
[12] CAO Y, JI Y, SUN Y, et al. The fault diagnosis of a switch machine based on deep random forest fusion. IEEE Intelligent Transportation Systems Magazine, 2023, 15(1): 437-452.
[13] SUN Y, CAO Y, LIU H, et al. Condition monitoring and fault diagnosis strategy of railway point machines using vibration signals. Transportation Safety and Environment, 2023, 5(2): tdac048.
[14] DRAGOMIRETSKIY K, ZOSSO D. Variational mode decomposition. IEEE Transactions on Signal Processing, 2014, 62(3): 531-544.
[15] HUANG N E, SHEN Z, LONG S R, et al. The empirical mode decomposition and the Hilbert spectrum for nonlinear and non-stationary time series analysis. Proceedings of the Royal Society of London. Series A: Mathematical, Physical and Engineering Sciences, 1998, 454(1971): 903-995.
[16] WEI H, QI T, FENG G, et al. Comparative research on noise reduction of transient electromagnetic signals based on empirical mode decomposition and variational mode decomposition. Radio Science, 2021, 56(10): e2020RS007135.
[17] SUN Y, LI S, WANG X. Bearing fault diagnosis based on EMD and improved Chebyshev distance in SDP image. Measurement, 2021, 176: 109100.
[18] GU Y, ZENG L, QIU G. Bearing fault diagnosis with varying conditions using angular domain resampling technology, SDP and DCNN. Measurement, 2020, 156: 107616.
[19] ZHANG S, ZHU X, XU Z. Research of motor bearing fault diagnosis based on deep belief network and symmetric dot pattern. Noise and Vibration Control, 2022, 42(3): 98-104
[20] YUAN H, CHEN J, YOU X, et al. Fault diagnosis of bearing in PMSM based on calibrated stator current residual signal and improved symmetrized dot pattern. IEEE Sensors Journal, 2024, 24(3): 3232-3246.
[21] WANG H. Fault diagnosis of reciprocating compressors based on VMD-SDP fusion image and CNN. Noise and Vibration Control, 2023, 43(4): 116-121.
[22] YE Z, YU J. Feature extraction of gearbox vibration signals based on multi-channels weighted convolutional neural network. Journal of Mechanical Engineering, 2021, 57(1): 110-120.
[23] LÜ S, GU L, GENG B. A recognition method of valve plate wear states of piston pump based on optimized VMD-CWT-CNN. Journal of Measurement Science and Instrumentation, 2024, 15(1): 43-53.
[24] ZHANG P, ZHANG G, DONG W, et al. Fault diagnosis of high-speed railway turnout based on convolutional neural network//2018 24th International Conference on Automation and Computing (ICAC), September 6-7, 2018, Newcastle Upon Tyne, UK. New York: IEEE, 2018: 1-6.
[25] WANG M, WANG H, DONG, et al. A method of compound fault signal separation based on EVMD-LNMF. Journal of Vibration and Shock, 2019, 38(16): 146-152.
[26] CHENG J, YU D, YANG Y. Research on the intrinsic mode function (IMF) criterion in EMD method. Mechanical Systems and Signal Processing, 2006, 20(4): 817-824.
[27] PICKOVER C. A. On the use of symmetrized dot patterns for the visual characterization of speech waveforms and other sampled data. The Journal of the Acoustical Society of America, 1986, 80(3): 955-960.
[28] LECUN Y, BOTTOU L, BENGIO Y, et al. Gradient-based learning applied to document recognition. Proceedings of the IEEE, 1998, 86(11): 2278-2324.
[29] LUO X, LU W, YOU Y, et al. A method for ball mill vibration signal random noise suppression based on VMD and SVD. Noise and Vibration Control, 2019, 39(6): 169-175.
[30] LIU S, FENG G, TANG J, et al. Research on identification of wood species by mid-infrared spectroscopy based on CA-SDP-DenseNet. Spectroscopy and Spectral Analysis, 2023, 43(3): 814-822.
[31] ZHU K, WANG J, LIU Y. Radar target recognition algorithm based on data augmentation and WACGAN with a limited training data. Acta Electronica Sinica, 2020, 48(6): 1124-1131.
[32] VAN DER MAATEN L, HINTON G. Visualizing data using t-SNE. Journal of Machine Learning Research, 2008, 9(11): 2579-2605.

基于VMD-SDP-CNN的铁路转辙机故障诊断

宋雅坤[1], 冯庆胜[1], 肖　帅[1], 李　红[2*]

1. 大连交通大学 电气工程学院, 辽宁 大连 116028;
2. 大连交通大学 轨道智能工程学院, 辽宁 大连 116028

摘　要： 转辙机是铁路系统中的重要设备, 对列车安全运行有着重要意义。针对现有转辙机故障诊断方法存在的问题, 并结合振动信号抗干扰性强及灵敏度高的特性, 本文提出一种基于转辙机振动信号的变分模态分解-对称点图像-卷积神经网络(Variational mode decomposition-symmetric dot pattern-convolutional neural network, VMD-SDP-CNN)故障诊断方法。实验中采集了ZD6转辙机的5种实际工况的振动信号作为研究对象。首先, 通过c对转辙机的振动信号进行分解, 得到多个本征模态函数(Intrinsic mode function, IMF)分量。其次, 采用对称点图案(Symmetric dot pattern, SDP)方法将分解的IMF分量转换为二维图像, 将一维信号识别问题转化为二维图像识别问题。最后, 利用卷积神经网络(Convolutional neural network, CNN)实现转辙机的故障诊断。实验结果表明, 使用该方法对转辙机5种实际工况的诊断效果优于典型深度学习和机器学习方法, 验证了其实用性和有效性。

关键词： 转辙机; 轨道交通; 道岔; 智能诊断; 振动信号; 信号分解; 深度学习

引用格式： SONG Yakun, FENG Qingsheng, XIAO Shuai, et al. Fault diagnosis of railway switch machines based on VMD-SDP-CNN. Journal of Measurement Science and Instrumentation, 2025, 16(2): 291-301. DOI: 10.62756/jmsi. 1674-8042.2025028